Sensors and Materials, Vol. 18, No. 7 (2006) 353–366
MYU Tokyo

S & M 0655

Plasma-Polymerized Allylamine-Based Label-Free Piezoelectric Immunosensor Platform: Characterization and Application

Andri Papadopoulou-Bouraoui, Josefa Barrero-Moreno*, Michael Lejeune, Frédéric Brétagnol, Miguel Manso, Andrea Valsesia, Pascal Colpo, Douglas Gilliland, Giacomo Ceccone and François Rossi

European Commission, Joint Research Centre, Institute for Health and Consumer Protection, Via Enrico Fermi - I-21020 Ispra (VA), Italy

(Received July 26, 2006; accepted September 8, 2006)

Key words: quartz crystal microbalance (QCM), immunosensor, plasma, surface characterization, gold nanoparticle (GNP)

During this study, a polyallylamine (ALL)-based label-free piezoelectric immunoprobe using a quartz crystal microbalance (QCM) was developed. Two routes for antibody (Ab) immobilization were investigated; the first involved the use of glutaraldehyde (GA) as a cross-linker and the second the use of colloid gold nanoparticles (GNPs) for surface amplification. The latter route, in combination with the use of an orienting protein, was further used in developing an immunosensor for an allergenic protein, ovalbumin (OVA). Surface characterization information on all the steps involved in the fabrication of the immunoprobe is provided in this paper. A combination of techniques such as imaging ellipsometry, atomic force microscopy (AFM), time-of-flight secondary ion mass spectrometry (TOF-SIMS) and X-ray photoelectron spectroscopy (XPS) was used for the characterization of the intermediate and final surfaces. Active amino groups were provided through the plasma deposition of ALL on a quartz crystal surface and further utilized for Ab immobilization. Results from this study show that simple, direct piezoelectric immunoprobes can be fabricated through appropriate Ab orientation and surface amplification techniques without the need for labeled compounds. The combination of surface analytical, optical, and mass characterization techniques confirms the effectiveness of these immunosensor fabrication strategies, whose analytical capacities can be extended to detect target molecules with matched antibodies.

*Corresponding author, e-mail address: josefa.barrero-moreno@jrc.it

1. Introduction

Label-free techniques for immunoassay-based devices are known to be advantageous in terms of simplicity of performance and saving time but often lack sensitivity compared with label-based methods. The sensitivity can however be improved by techniques allowing active surface amplification and appropriate antibody (Ab) orientation for immunoreaction enhancement.

In recent years, gold nanoparticles (GNPs) deposited on transducer surfaces have been increasingly used in biological applications because of their good biocompatibility and large surface area compared with flat surfaces.[1,2] Although colloidal gold does not harm the nature of proteins,[3] the direct adsorption of proteins on gold surfaces can cause denaturation and the loss of their bioactivity. Hydrogels such as poly (acrylamide) as well as self-assembled monolayers (SAMs) formed by thiols have been utilized for the immobilization of GNPs on surfaces. However, the shrinking and swelling of the hydrogels and malodorous nature of the thiols are some of the disadvantages associated with these methods compared with those using plasma-polymerized organic amines such as propylamine,[4] aminosilanes,[5] or n-butyl amine.[6] Plasma polymers have the advantage of providing a good coverage on a wide range of surfaces and of being pinhole-free.

Choosing an Ab immobilization strategy is a key process for successful immunosensing device development, and for improving sensitivity and reproducibility. Controlled orientation methods of Ab immobilization through its Fc region can be performed using protein A (PA)[7] and protein G (PG), which are cell wall proteins from *Staphylococcus aureus* and *Streptococcus sp.* recombinant *Escherichia coli*, respectively, because of their natural affinity for the Fc region of IgG molecules.[6]

In this study, we have made use of these orienting proteins combined with the cross-linking capacity of glutaraldehyde (GA),[8] or the surface amplification capacity of gold nanoparticles (GNPs).[6,8,9] A schematic presentation of the two routes, as well as the reaction mechanism for Ab immobilization and the Ab-antigen reaction for the cross-linking in the GA route are shown in Fig. 1. Both routes were investigated on plasma-deposited polyallylamine (ALL) as a surface amine group provider used for the further development of a piezoelectric immunoprobe.

A quartz crystal microbalance (QCM) was used during this study for the detection method. The method is a mass-sensitive technique that allows the measurement of the resonance frequency shift (ΔF) attributed to changes in the total oscillating mass of the crystal. Advantages associated with this technique are its simple operation and high sensitivity. The piezoelectricity concept was first introduced by Rayleigh in 1885, but it was not until 1959, when Sauerbrey[10] presented his equation relating frequency to mass, that piezoelectricity (eq. 1) was used for chemical sensor development.

$$\Delta F = -2\frac{F_0^{\,2}}{\sqrt{\rho_q \mu_q}}\frac{\Delta m}{A} \tag{1}$$

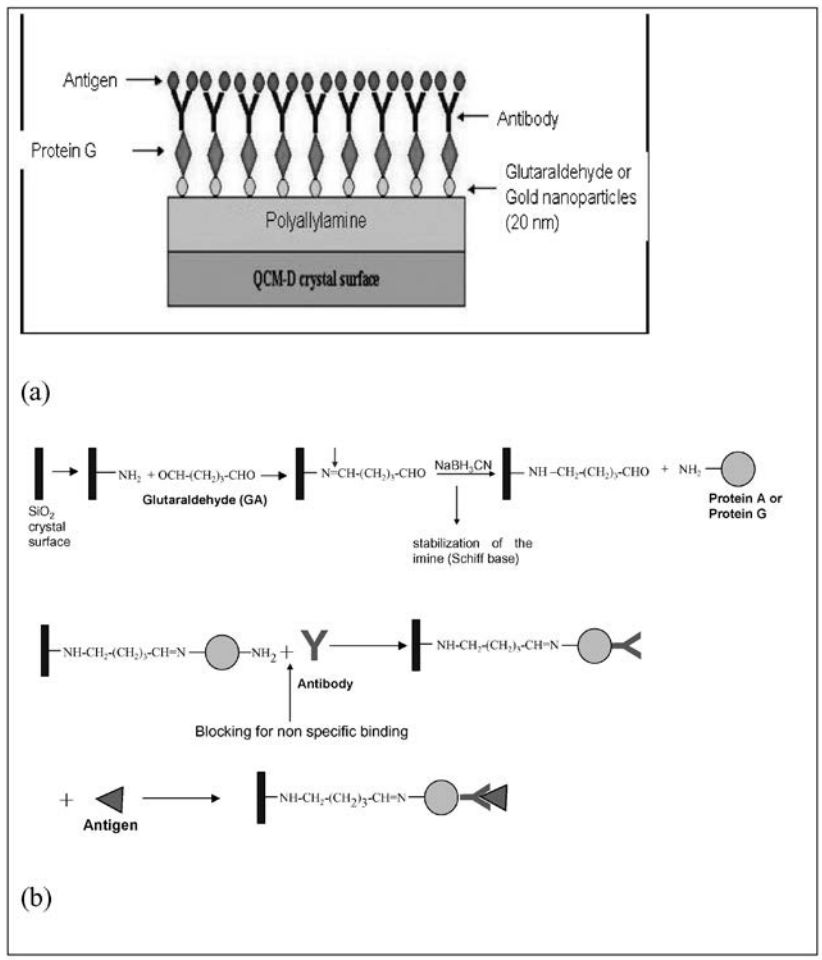

Fig. 1. (a) Proposed direct, label-free immunosensor schemes and (b) reaction mechanism schematic for Ab immobilization and Ab-antigen reaction for cross-linking in GA route.

Here, Δm is the change in the mass on the sensor surface, F_0 is the fundamental frequency, A is the electrode surface area, and ρ_q and μ_q are the density and the shear modulus of the quartz crystal, respectively. The Sauerbrey equation assumes that mass is uniformly distributed as a rigid elastic thin film. This is the case for gas phase deposition. When operating in liquid, bulk liquid properties such as conductivity, viscosity, density and dielectric constant should be taken into account for the interpretation of ΔF.[11,12] In the case of a thin layer and high frequency resulting from an immunoreaction, the antibody or antigen behaves like a glassy material. The viscoelastic effect is therefore negligible and the Sauerbrey equation could be used in this case.[13]

The possibility of using this technique in liquid has enabled its application to the sensitive detection of many compounds such as pesticides,[14–16] polyaromatic hydrocarbons, viruses,[17] bacteria,[18,19] or proteins such as human serum albumin for the diagnosis of renal disease in diabetic patients.[13] The simplicity of design and the use of the label-free direct assay formats are important advantages in the QCM sensor design, especially for the detection of compounds of large molecular weight. Appropriate blocking for nonspecific binding and the use of purified biomolecules can overcome some of the problems associated with this label-free direct assay format.[20]

A step-by-step surface characterization of the immunosensor was performed with a combination of surface analytical and optical techniques such as X-ray photoelectron spectroscopy (XPS), time-of-flight secondary ion mass spectrometry (TOF-SIMS), ellipsometry, and atomic force microscopy (AFM). The QCM technique allowed the 'real-time' deposition and stability monitoring of the steps associated with Ab immobilization and the immunoreaction.

This system has been tested for the detection of ovalbumin (OVA). OVA is a major egg allergen and the most common immunological method available for its detection in food is the enzyme-linked immunosorbent assay (ELISA). Piezoelectric immunosensors do not exist for the detection of OVA. For this reason the immunoprobe fabricated was used to test the reaction between the monoclonal anti-ovalbumin (anti-OVA) and OVA.

2. Materials and Methods

2.1 *Reagents and materials*

An allylamine precursor, trifluoromethylbenzaldehyde (TFMB), phosphate buffered saline (PBS), a GA solution (50%), the anti-OVA, OVA, bovine serum albumin (BSA), a colloidal gold suspension (20 nm), PG from *Streptococcus sp.* recombinant *E.coli* walls and Tween 20® were obtained from Sigma Aldrich (Milan, Italy).

2.2 *Allylamine plasma deposition*

ALL films were deposited in a cylindrical, capacitively coupled plasma reactor. The experiment is described in ref. 21. Briefly, Ar discharge was maintained using a radio frequency (RF) power supply (13.56 MHz) (Dressler Integro 133) powered at 20 W for 20 min with the pressure set at 45 mTorr, an Ar flow of 6 sccm and an equivalent ALL flow of 12 sccm. Deposition was performed on a SiO_2-covered gold surface of AT-cut 5-MHz QCM-D quartz crystals for further development into a piezoelectric immunosensor, or on a Si surface for XPS, TOF-SIMS, ellipsometry, and AFM characterization.

2.3 *Surface characterization by XPS, TOF-SIMS, ellipsometry and AFM*

An axis ultra spectrometer (KRATOS, Analytical, Manchester, UK) equipped with a monochromatic A1 150 W ($h\nu$ = 1486.6 eV) source, operating at 150 W was used for XPS analysis. The presence and quantity of active primary amine groups provided by the ALL film were investigated by an XPS analysis of the derivative formed by exposure to TFMB in the gas phase at 45°C. The reaction mechanism[22,23] is shown in Fig. 2.

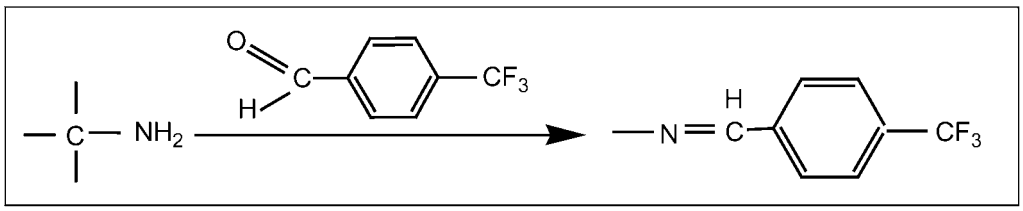

Fig. 2. Derivatization reaction for determination of primary amine groups (-NH_2) by XPS analysis.

According to the reaction mechanism, one NH_2 group is substituted by a C=N bond, and CF_3 terminal bonds appear, with a one-to-one ratio between CF_3 and NH_2. The derivatized ALL layers were washed with water prior to XPS analysis. The NH_2 density was calculated using the relationship below (eq. 2), which takes into account the additional C introduced by the TFMB molecules.[22]

$$\left[\mathrm{NH_2}\right] = \left[\frac{[F]}{3} / \left([C] - 8\frac{[F]}{3}\right)\right] \times 100\% \tag{2}$$

Here, [*F*] and [*C*] are the fluorine and carbon concentrations determined by XPS respectively after the reaction with the TFMB.

TOF-SIMS analysis was performed using an ION-TOF IV spectrometer (Munster, Germany). AFM experiments were performed using the intermittent-contact mode on a Solver instrument equipped with a Smena head (NT-MDT, Moscow, Russia). The cantilever was a standard silicon cantilever (NT-MDT) (resonance frequency ν_{res} = 150 KHz), equipped with a tip characterized by an aspect ratio of 1:10. Quantitative analysis of the images was carried out by the SPIP software provided by Image Metrology A/S (Lyngby, Denmark). Ellipsometry measurement was performed using an imaging ellipsometer from Nanofilm Technology GmbH (Göttingen, Germany).

2.4 *Quartz crystal microbalance (QCM)*

The 'real-time' monitorings of film stability and of all the subsequent steps (orienting protein adsorption, Ab loading and Ab-antigen reaction) were performed using a QCM equipped with a dissipation monitor (QCM-D, Q-Sense, Gothenburg, Sweden). Oscillating Δ*F*s were detected and plotted in real time at a resonant frequency of 5 MHz and at the 15, 25, and 35 MHz overtones. ALL films were deposited on the AT-cut 5 MHz quartz crystal covered with Au and SiO_2 layers. The active electrode area of the QCM crystals used was 0.3 cm^2. The QCM was shown to have sensitivity at the ng·cm^{-2} level. All measurements were performed at 25°C.

2.5 *Antibody immobilization process and immunoreaction monitoring*

Two different Ab immobilization routes were investigated. The first involved the use of GA as a cross-linker (2.5% in PBS pH 7.4), followed by PG in PBS, pH 6.0 for optimal

orientation of the anti-OVA on the ALL surface. In the second route, nanometer-sized (20 nm) GNPs, in combination with PG were used for surface amplification. The ALL-coated crystals were incubated with 200 μL of GNPs for 4 h at 4°C.

The unstable Schiff base produced by the reaction between the active primary amine groups and the aldehyde function of GA was stabilized using sodium cyanoborohydrate to reduce the double bond of the imine formed between the primary amine group and the aldehyde function of GA. The blocking of unreacted, free amine groups was performed using 1% BSA in PBS containing 0.05% Tween 20® (PBST). The immunoreaction was tested by placing 200 μL of standard solutions containing OVA in the 2 to 20 mg/mL range in contact with the immunoprobe surface containing the immobilized specific Ab.

3. Results and Discussion

3.1 *QCM results*

The piezoelectric platform was first coated with plasma-deposited ALL to provide amine groups at the surface for further development of the piezoelectric immunoprobe. Next, we studied two strategies of Ab immobilization. In the first method, an orienting protein (PG) combined with the cross-linking capacity of GA was used, whereas in the other strategy, the surface amplification capacity of GNPs deposited on NH_2-terminated surfaces was used.

All the main intermediate steps in the Ab immobilization as well as the Ab-antigen reaction were monitored in 'real time' using the QCM. The two Ab immobilization routes were compared using the QCM for the ΔF's due to orienting protein and Ab loadings as well as for the ΔF's due to the blocking step and Ab-antigen reaction sensitivity. Figure 3 shows the ΔF in Hz for all the major steps involved using the two routes. It can be observed that the GNP route resulted in a higher ΔF due to the Ab loading, even though a lower ΔF was initially observed for the orienting protein immobilization. It can thus be concluded that GNPs have a positive role in Ab loading and the sensitivity of the immunoreaction. This may be attributed to the increase in surface roughness and consequently the surface amplification resulting from the presence of the GNPs on the ALL surface. As a consequence of the more important Ab loading, antigen loading was higher for the GNP route. The differences obtained in ΔF for each step from the two immobilization routes are compatible with the findings from the ellipsometry and AFM studies as discussed below.

The immunoprobe fabricated through the GNP route was used to test the reaction between the anti-OVA and OVA. Figure 4 shows the F curves for the 15, 25, and 35 MHz overtones obtained for PG and the anti-OVA loadings.

OVA concentrations from 2 to 20 mg/ml were tested, and the F curves for the 35 MHz overtone for the OVA addition are shown in Fig. 5(a), where a gradual decrease in the frequency is observed until equilibrium is reached. As can be seen from Fig. 5(b), a high correlation coefficient ($R^2 = 0.987$) is obtained between the QCM signal and the OVA concentration. Blank samples were also prepared by immobilizing the Ab directly onto the SiO_2 surface of the quartz crystal and were tested for using the 10 mg/mL OVA solution. The final Ab-antigen reaction was observed on the blank SiO_2 surface for the 10 mg/mL OVA solution tested, but at a lower intensity, and lacked repeatability. This confirms the

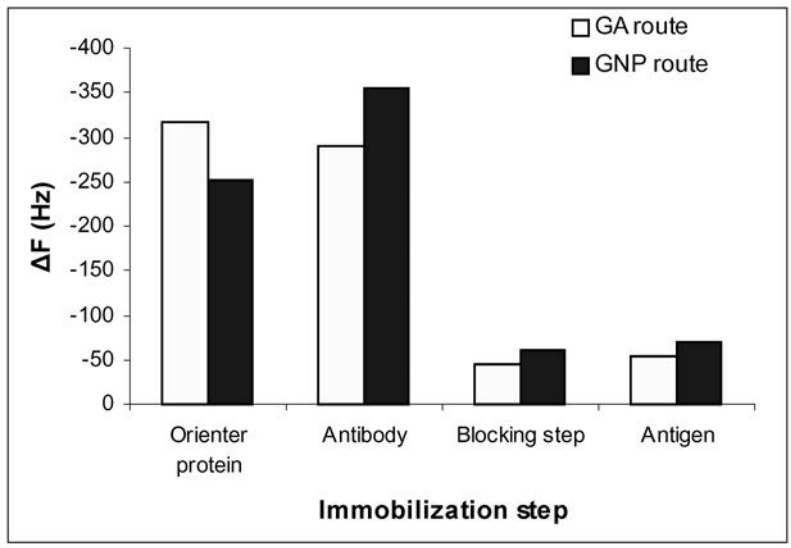

Fig. 3. D*F*'s attributed to each immobilization step for two Ab immobilization routes studied.

role of the orienting protein, showing that when the Ab is not correctly oriented, its antigen binding sites are not always completely available for obtaining the most sensitive reaction.

3.2 *Ellipsometry and AFM measurements*

Ellipsometry allowed the large-scale imaging of the various layers and provided information about their thicknesses, which are shown in Table 1. It can be seen that even though for the GA route, a thicker layer of the orienting protein is formed in comparison with the GNP route, the subsequent Ab layer is considerably less thick (d = 34 nm vs 87 nm). Furthermore, the GA method resulted in a smoother orienting protein surface, whereas the rougher orienting protein surface in the GNP method clearly favors Ab loading. This was confirmed by the AFM images shown in Fig. 6. Results obtained for the GNP layer using the AFM technique are shown in Fig. 6(a). It can be seen that the GNPs formed a monolayer topped by micrometric randomly distributed clusters. GNP attachment is achieved through electrostatic forces, since ALL is positively charged and GNPs are negatively charged. The effect of deposition time for the GNPs on the bare ALL surface was studied by incubating the GNPs for 4 and 12 h. After 12 h of incubation, larger clusters were observed compared with the smaller, more regularly distributed clusters observed after 4 h of incubation. An incubation of 4 h was therefore used for all subsequent experiments to ensure a more regular distribution of GNPs. Figures 6(b) and 6(c) show that at equal scales (2.5×2.5 μm), a noticeable difference is visible between the two images, with the GNP route resulting in larger Ab clusters. The initial ALL film roughness (RMS) was found to be less than 2 nm in both cases. The RMS of the ALL film functionalized with GNPs increased to 9.02 nm, whereas that of ALL-GA film was 0.8 nm. The surface area ratio increased in the case of ALL-GNP film by 13.3%, whereas that change was equal to

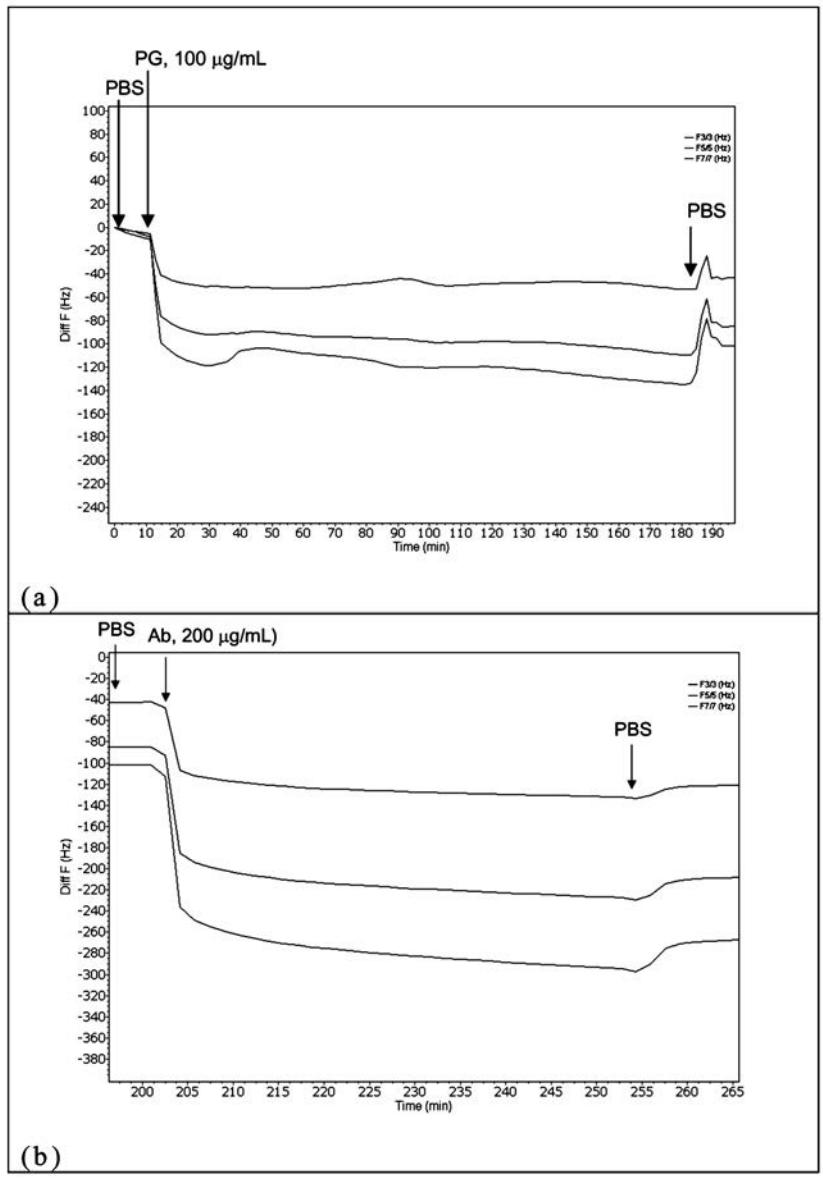

Fig. 4. (a) PG and (b) Ab-loading monitoring using QCM. F3/3, F5/5 and F7/7 correspond to the 15, 25, and 35 MHz overtones.

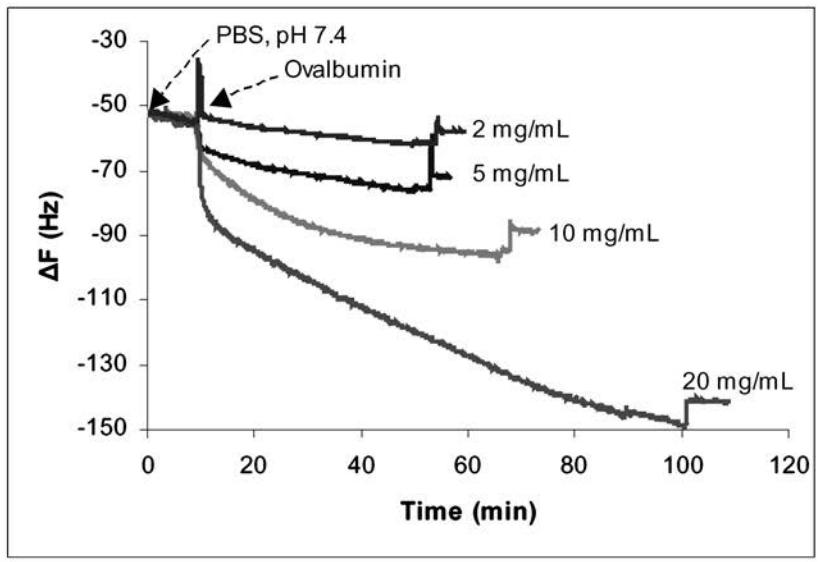

(a)

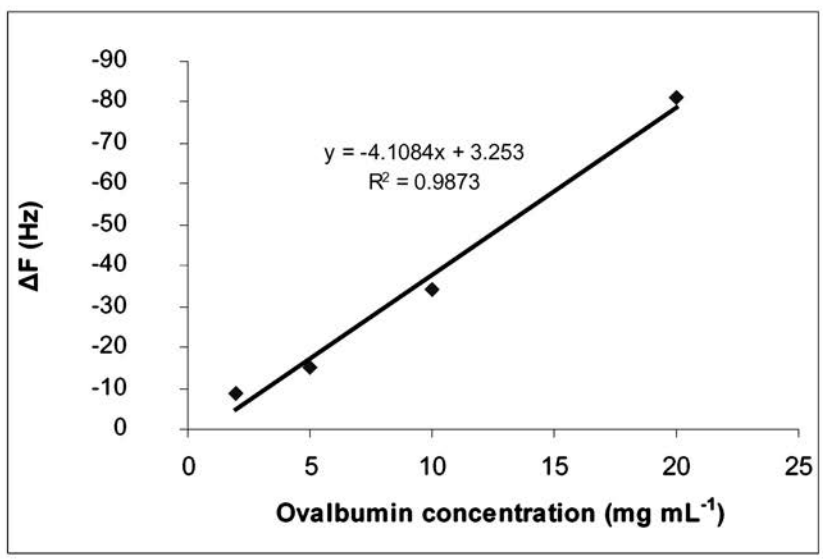

(b)

Fig. 5. (a) Δ*F* curves due to Ab-antigen reaction (anti-OVA-OVA) for several concentrations using GNP-based immunoprobe and (b) linear regression between Δ*F* and OVA concentration.

Table 1
Thicknesses of added layers as determined by ellipsometry.

Layer thickness (*d*) (nm)	GA-orienting protein	GNP- orienting protein
ALL	319	319
GNP	–	7
GA+$NaBH_3CN$	18	–
Orienting protein	84	21
Ab	34	87

0.055% for the ALL-GA film. These findings are related to the ellipsometry findings, as well as to the higher-Ab loading found using the GNP method as determined by the QCM.

3.3 *XPS results*

The characterization of the ALL film was performed by XPS. According to the XPS analysis, ALL deposition resulted in an N/C ratio of 0.23, whereas the oxygen content was below 7% with an O/C ratio of 0.08. These figures are comparable with those reported in the literature.[24,25] The C1s fitting showed the presence of C-N and CNO bonds and some COOR functionalities.[21,26] Figure 7 shows the high-resolution spectra of the ALL films. The C1s spectrum of the sample derivatized using TFMB shows the presence of 292.88 CF_3 compounds, indicating the appearance of derivatized primary amine groups with an activity of about 2%, which is comparable to the values found in the literature for other RF plasma processes.[27]

The N/C and O/C ratios from XPS analysis for both immobilization schemes are shown in Table 2. Quantitative analysis of the ALL-GA sample indicated a decrease in the N/C ratio (to 0.21) and an increase in the O/C ratio (to 0.13). This shows that GA is successfully immobilized on the ALL surface. In the GNP route, the addition of GNPs (8% atomic concentration) led to a decrease in the N/C ratio, whereas the O/C ratio increased slightly. Concerning the characterization of the orienting protein layer, quantitative analysis indicated that the N/C ratio decreased to 0.19. To obtain evidence for its presence, the orienting protein was deposited directly on the Si surface covered with gold or ALL. The orienting protein deposited on Au resulted in an N/C ratio of 0.13, whereas when it was immobilized directly on the ALL film, this ratio was 0.23. This, as well as the similarity of the C1s spectra of the ALL-GA-orienting and Au-orienting proteins, are indications of the successful immobilization of the orienting protein onto the functionalized surfaces. The Ab immobilization, on the other hand, cannot univocally be determined by XPS without the use of labelled compounds, since the N/C ratio after this step remains very similar to the N/C ratio of the ALL film.

3.4 *TOF-SIMS results*

TOF-SIMS spectra provided information about each immobilization step. The ion fragments for the characterization of the ALL and ALL-GA-$NaBH_3CN$ layers are shown in Fig. 8.

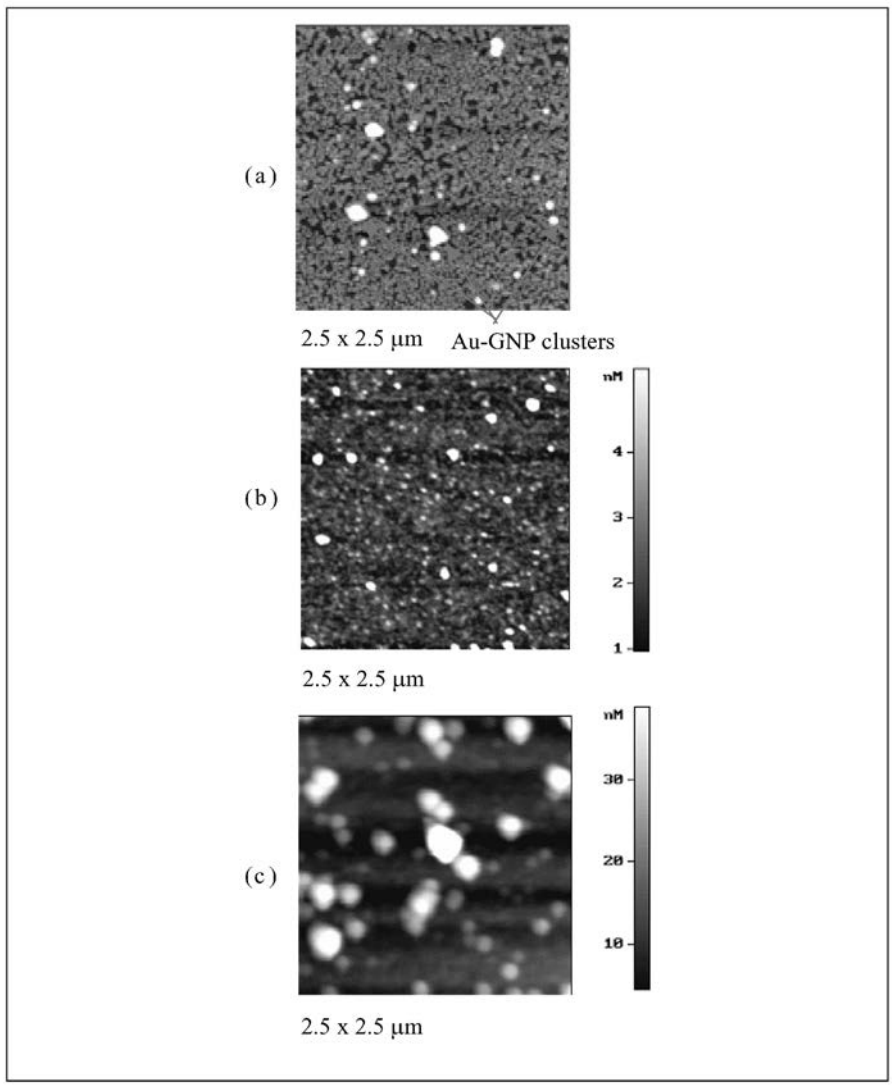

Fig. 6. AFM images showing (a) GNP layer; (b) and (c) Ab adsorption for the two routes studied.

Positive identification of the GA layer on the ALL film was possible through TOF-SIMS analysis, because of the increase in the intensity of fragments such as the CH_3O, C_2H_5O and C_3H_7O fragments, whose intensities are much lower in spectra from the ALL layer (Fig. 8(a)). Increases in the peak areas are indicative of the presence of amino acid ion fractions such as methionine (C_2H_5S), serine ($C_3H_3O_2$) and leucine ($C_5H_{12}N$), and, thus, indicate of the presence of the orienting protein.

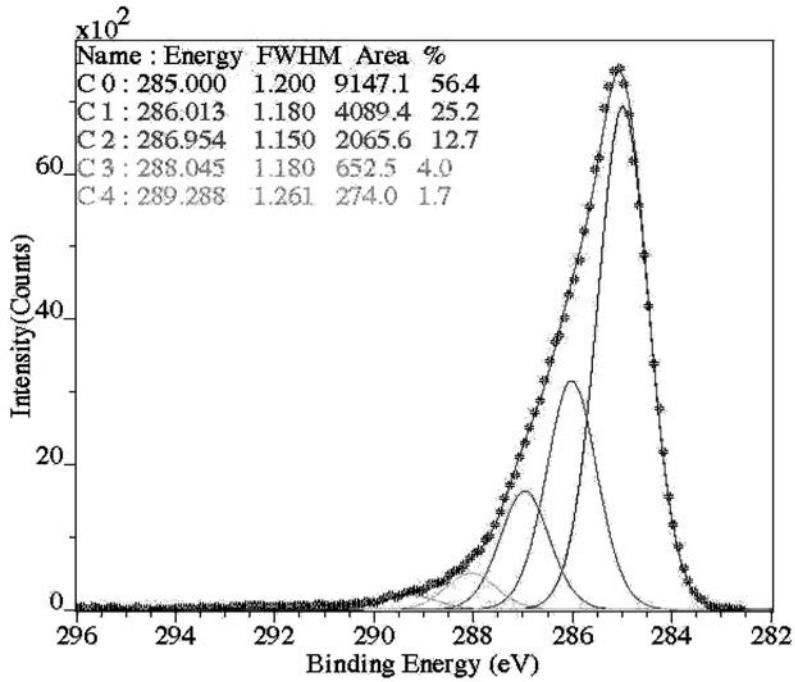

Fig. 7. XPS C1s high-resolution spectra of ALL films.

Table 2
N/C and O/C ratios from XPS analysis for each stage of each route for Ab immobilization.

GA-route		
Immobilization step	N/C ratio	O/C ratio
ALL	0.23	0.08
GA	0.21	0.13
$NaCNBH_3$	0.22	0.11
Orienting protein	0.19	0.29
Ab	0.22	0.22
GNP-route		
Immobilization step	N/C ratio	O/C ratio
ALL	0.23	0.08
GNP	0.18	0.12
Orienting protein	0.19	0.30
Ab	0.21	0.22

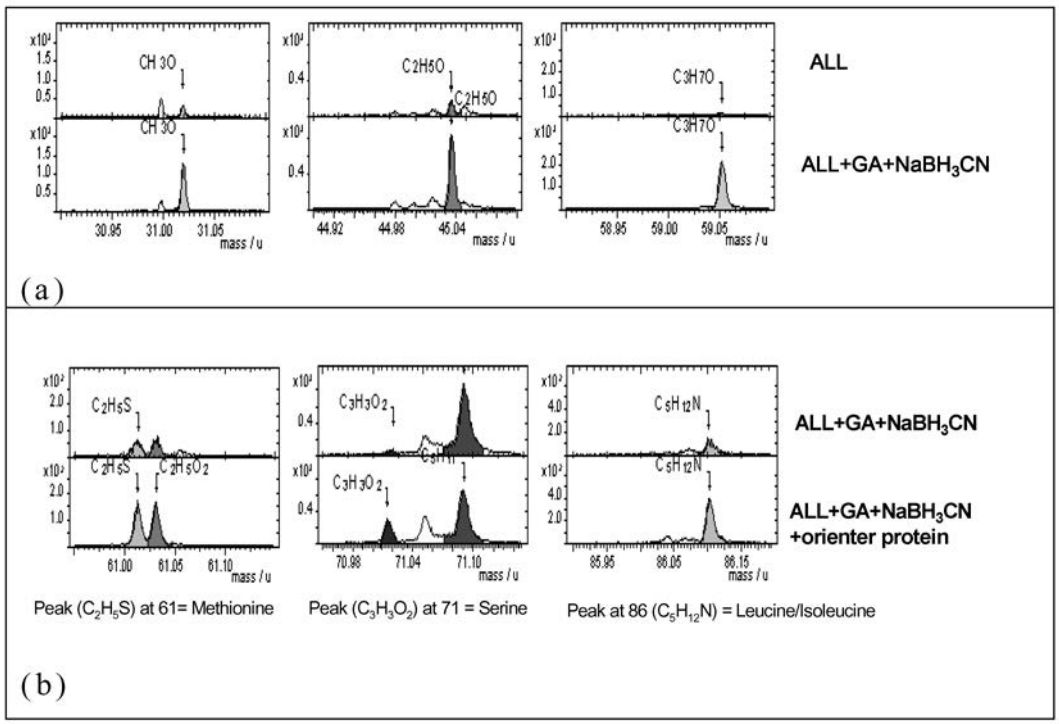

Fig. 8. Ion fragments from TOF-SIMS analysis: (a) ion fragments showing the presence of GA and (b) ion fragments attributed to the presence of the orienting protein on the ALL-GA-$NaBH_3CN$ layer.

4. Conclusion

The fabrication of a simple, direct label-free piezoelectric immunoprobe, utilizing an orienting protein (PG) for the optimum orientation of the Ab was proposed. The plasma-modified surface created by ALL was an optimum pinhole-free source of active amine groups for further use in Ab immobilization. It was demonstrated that the use of GNPs is a more efficient way for immobilizing Abs than the direct chemical method utilizing GA, because of their capacity to increase the available active area. Through the combination of surface characterization techniques, it was possible to find evidence of the presence of each active layer. The use of QCM provides a simple piezoelectric transducer able to monitor in real time the adlayers for surface functionalization towards immunosensor development as proposed here, and to monitor the Ab-antigen reactions functioning as a simple immunosensing device. The possibility of the application of this direct method for the determination of a major food allergen, OVA, was demonstrated using standard concentrations of OVA. Considering that food allergies affect 1–3% of the adult population and 4–6% of children, and that food-induced symptoms affect 22% of the population, this direct piezoelectric immunosensor platform is a promising technique for the efficient and rapid determination of this food allergen, or other Ab-antigen couples as an alternative to

immunoenzymatic or chromatographic techniques. The European Commission Regulation 2000/13/EC[28] and its amendment 2003/89/EC[29] imposed by Member States on October 11, 2004, makes obligatory the labeling of all ingredients. The direct piezoelectric platform presented here could therefore be a simple means of detecting high-molecular-weight molecules such as food allergenic proteins.

References

1 J. J. Storhoff, R. Elahanian, R. C. Mucic, C. A. Mirkin and R. L. Lestinger: J. Am. Chem. Soc. **120** (1998) 1959.
2 A. L. Crumbliss, S. C. Perine, J. Stonehunerer, K. R. Tubergen, J. G. Zhao, R. W. Henkens and J. P. O'daly: Biotechnol. Bioeng. **40** (1992) 483.
3 C. R. Martin and D. T. Micher: Anal. Chem. **70** (1998) 322A.
4 F. Fally, C. Doneux, J. Riga and J. J. Verbist: J. Appl. Polym. Sci. **56** (1995) 597.
5 J. Ida, T. Matsuyama and H. J. Yamamoto: Electrost. **49** (2000) 71.
6 W. Wang, Y. Liu, Y. Yang, T. Deng, G. Shen and R. Yu: Anal. Biochem. **324** (2004) 219.
7 S. Babacan, P. Pivarnik, S. Letcher and A. G. Rand: Biosens. Bioelectron. **15** (2000) 615.
8 M. Wang, L. Wang, G. Wang, X. Ji, Y. Bai, T. Li, S. Gong and J. Li: Biosens. Bioelectron. **19** (2004) 575.
9 Y. Liu, L. Li, Y. Liu and S. Yao: Biomaterials **25** (2004) 5725.
10 G. Sauerbrey: Zeitschrift Fur Physik **155** (1959) 206 (in German).
11 R. Bruckenstein and M. Shay: Electrochim. Acta **30** (1985) 1295.
12 K. K. Kanazawa and J. G. Gordon: Anal. Chem. **57** (1985) 1771.
13 S. P. Sakti, P. Hauptmann, B. Zimmermann, F. Buhling and S. Ansorge: Sens. Actuators, B **78** (2001) 257.
14 G. G. Guibault, B. Hock and R. Schmid: Biosens. Bioelectron. **7** (1992) 411.
15 J. Horacek and P. Skladal: Anal. Chim. Acta **347** (1997) 43.
16 C. Steegborn and P. Skladal: Biosens. Bioelectron. **12** (1997) 19.
17 C. C. Su, T. Z. Wu, L. K. Chen, H. H. Yang and D. F. Tai: Anal. Chim. Acta **479** (2003) 117.
18 X. L. Su and Y. Li: Biosens. Bioelectron. **19** (2004) 563.
19 X. L. Su and Y. Li: Biosens. Bioelectron. **21** (2005) 840.
20 X. Su, F. T. Chew and F. Y. Li: Anal. Sci. **16** (2000) 107.
21 F. Bretagnol, L. Ceriotti, M. Lejeune, A. P.-Bouraoui, M. Hasiwa, D. Gilliland, G. Ceccone, P. Colpo and F. Rossi: Plasma Process Polym. **3** (2006) 30.
22 A. Choukourov, J. Kousal, D. Slavinska, H. Biederman, E. Fuoco, S. Tepavcevic, J. Saucedo and L. Hanley: Vacuum **75** (2004) 195.
23 F. Palmisano, G. E. De Benedetto and C. G. Zambonin: Analyst **122** (1997) 365.
24 I. Gancarz, G. Pozniak, M. Bryjak and W. Tylus: Eur. Polym. J. **38** (2002) 1937.
25 I. Gancarz, G. Pozniak, M. Bryjak and W. Tylus: Eur. Polym. J. **38** (2003) 2217.
26 M. Tatoulian, F. Bretagnol, F. A.-Khosari, J. Amouroux, O. Bouloussa, F. Rondelez, A. J. Paul and R. Mitchell: Plasma Process Polym. **2** (2005) 38.
27 A. A. M.-Plath, K. Schroeder, B. Finke and A. Ohl: Vacuum **71** (2003) 391.
28 European Commission: Official Journal of the European Communities L109/29. Directive 2000/13/EC (2000).
29 European Commission: Official Journal of the European Communities L308/15. Directive 2003/89/EC (2003).